Biochemical and Biophysical Research Communications 827 (2026) 154001

Contents lists available at ScienceDirect

Biochemical and Biophysical Research Communications

journal homepage: www.elsevier.com/locate/ybbrc

Staphylococcus aureus activates dendrite elongation in dendritic cells

Kai Kobata, Kazuyuki Furuta *, Yuki Ikeya, Yohei Chishaki, Kazuya Ishikawa, Chikara Kaito

Graduate School of Medicine, Dentistry, and Pharmaceutical Sciences, Okayama University, Japan

ARTICLE INFO

Keywords:
Staphylococcus aureus
Dendritic cells
Dendrite elongation
Peptidoglycan: TLR2/MyD88 signaling
ERK/PI3K/Cdc42 pathway
Short-chain fatty acids (SCFAs)
Butyrate
Host–microbe interactions
Antigen presentation
T-cell activation
IL-17
IL-10

ABSTRACT

Dendritic cells (DCs) are thought to extend dendrites to enhance the efficiency of antigen uptake and presentation. We previously reported that short-chain fatty acids (SCFAs), such as butyrate and valerate, promote dendrite extension in DCs. In this study, we found that the human pathogen *Staphylococcus aureus* also induces dendrite extension in DCs and investigated the underlying mechanisms. Dendrite extension in DC2.4 cells was induced not only by live *S. aureus* but also by heat-killed bacteria and purified peptidoglycan (PGN). DC2.4 cells lacking TLR2 or its adaptor protein MyD88 extend dendrites in response to SCFAs, but failed to extend dendrites in response to *S. aureus*. Furthermore, inhibitors of ERK, PI3K, and Cdc42 suppressed dendrite extension triggered by *S. aureus*. Co-stimulation with *S. aureus* and butyrate enhanced dendrite extension beyond either stimulus alone. DC2.4 cells co-stimulated with *S. aureus* and butyrate also showed increased uptake of insoluble beads and, upon co-culture with T cells, induced elevated production of IL-17 and IL-10 by T cells. Collectively, these findings suggest that *S. aureus* activates ERK/PI3K/Cdc42 signaling through TLR2 recognition of PGN to drive dendrite extension in DCs. In addition, *S. aureus* promotes dendrite extension in DCs *via* a pathway distinct from that of SCFAs, thereby acting cooperatively with SCFAs to enhance immune responses.

1. Introduction

Dendritic cells (DCs) are professional antigen-presenting cells that recognize and capture invading pathogens and present pathogen-derived antigens on major histocompatibility complex (MHC) molecules to T cells, thereby initiating adaptive immune responses [1,2]. Upon antigen presentation by DCs, naïve $CD4^+$ T cells differentiate into functional subsets such as Th1, Th2, Th17, regulatory T cells (Tregs), or T follicular helper (Tfh) cells, depending on the nature of DC–T cell interactions and the surrounding cytokine milieu [3,4]. Among the effector cytokines, IL-17 produced mainly by Th17 cells promotes neutrophil differentiation and migration and induces antimicrobial peptides, thereby contributing to protective responses against bacterial infection [5]. In contrast, IL-10 is produced by several T cell subsets, including Tregs, Th2 cells and certain subsets of Th1 and Th17 cells, and acts as an immunoregulatory cytokine that suppresses excessive inflammation at infection sites to prevent host tissue damage [6,7].

DCs are highly dynamic immune cells that continuously remodel their morphology to probe the surrounding environment and capture antigens. These morphological changes are thought to influence antigen uptake and subsequent T cell priming; however, the molecular mechanisms that regulate DC shape and function remain incompletely understood. We recently reported that short-chain fatty acids (SCFAs) such as butyrate, valerate, and propionate—microbial metabolites enriched in the gut—induce dendrite extension in DCs by inhibiting histone deacetylases (HDACs) [8]. We further demonstrated that SCFA-induced dendrite extension requires actin polymerization and activation of the Rho family small GTPase Cdc42 [8]. Cdc42 promotes actin polymerization through activation of WASP family proteins and the Arp2/3 complex, leading to the formation of filopodia and microspikes [9–11]. PI3K signaling locally activates Cdc42 and Rac1, thereby controlling actin remodeling and cellular morphology [12,13].

Although SCFAs have been identified as exogenous stimuli that promote dendrite extension, little is known about whether bacterial

Abbreviations: APC, antigen-presenting cell; CRMP2, collapsin response mediator protein 2; DC, dendritic cell; ERK, extracellular signal-regulated kinase; FBS, fetal bovine serum; HDAC, histone deacetylase; KD, knockdown; KO, knockout; MAPK, mitogen-activated protein kinase; MOI, multiplicity of infection; MyD88, myeloid differentiation primary response 88; OVA, ovalbumin; PGN, peptidoglycan; PI3K, phosphoinositide 3-kinase; PSM, phenol-soluble modulin; qPCR, quantitative polymerase chain reaction; SCFA, short-chain fatty acid; *S. aureus*, *Staphylococcus aureus*; TLR, Toll-like receptor.

* Corresponding author. 1-1-1 Tsushima-naka, Kita-ku, Okayama, 700-8530, Japan.
E-mail address: furutak@okayama-u.ac.jp (K. Furuta).

https://doi.org/10.1016/j.bbrc.2026.154001
Received 8 January 2026; Received in revised form 20 May 2026; Accepted 20 May 2026
Available online 25 May 2026
0006-291X/© 2026 The Authors. Published by Elsevier Inc. This is an open access article under the CC BY license (http://creativecommons.org/licenses/by/4.0/).

pathogens themselves can induce dendrite extension in DCs. In this study, we focused on *Staphylococcus aureus*, a representative human pathogen recognized by the innate immune system, and investigated its ability to promote dendrite extension. We found that peptidoglycan (PGN), a major cell wall component of *S. aureus*, triggers dendrite extension in DCs through TLR2 and its adaptor MyD88. Moreover, when DCs were co-stimulated with *S. aureus* and SCFAs, dendrite extension and DC-mediated T cell activation were further enhanced. These findings reveal that *S. aureus* activates dendrite extension and immune function via a pathway distinct from SCFAs, thereby acting cooperatively with butyrate to potentiate DC activation.

2. Experimental procedures

2.1. Reagents

The following reagents were used, with suppliers indicated in parentheses: fetal bovine serum (FBS; NICHIREI), RPMI-1640 medium (Fujifilm Wako Pure Chemical), penicillin–streptomycin solution (Fujifilm Wako Pure Chemical), cytochalasin B (Fujifilm Wako Pure Chemical), LPS (Sigma-Aldrich), peptidoglycan (Sigma-Aldrich), poly(I:C) (Sigma-Aldrich), CHIR99021 (Cayman Chemical), CK-666 (Cayman Chemical), SC-514 (Cayman Chemical), U0126 (Cayman Chemical), SP600125 (Cayman Chemical), SB203580 (Cayman Chemical), EHT1864 (Cayman Chemical), ML141 (Cayman Chemical), LY294002 (Cayman Chemical), Y27632 (Focus Biomolecules), FITC-labeled OVA (Thermo Fisher Scientific), Polyethylenimine "MAX" (PEI-MAX) (Polysciences), Fluoresbrite YG microspheres (1.0 μm; Polysciences), FITC anti-mouse H-2Kb antibody (clone AF6-88.5), FITC anti-mouse CD80 antibody (clone 16-10A1), PE anti-mouse CD274 (PD-L1) antibody (clone 10F.9G2), PE anti-mouse CD86 antibody (clone GL-1), APC anti-mouse I-Ab antibody (clone AF6-120.1), APC anti-mouse CD40 antibody (clone 3/23), sodium butyrate (Nacalai Tesque), and ELISA kits for mouse IFN-γ, IL-10, and IL-17 (BioLegend).

2.2. Cell culture

The murine dendritic cell line DC2.4, kindly provided by K. Rock (Dana-Farber Cancer Institute, Boston, MA, USA), was cultured in RPMI-1640 medium supplemented with 10% FBS, penicillin (0.1 mg/mL), streptomycin (100 U/mL) (referred to as RPMI-1640 medium throughout this manuscript), and 50 μM 2-mercaptoethanol. HEK293FT cells were cultured in DMEM supplemented with 10% FBS, penicillin (0.1 mg/mL), streptomycin (100 U/mL), and 50 μM 2-mercaptoethanol. All cells were maintained at 37 °C in a humidified incubator with 5% CO_2. BMDCs were prepared as previously reported [8]. Briefly, bone marrow cells were collected from the tibia and femur of B10.BR. mice. The cells were cultured in RPMI-1640 medium containing 10% FBS, 100 U/mL penicillin, 0.1 mg/mL streptomycin, and 50 μM β-mercaptoethanol in the presence of 10 ng/mL mouse GM-CSF at 37 °C in 5% CO_2 for 7–8 days.

2.3. Mice

Mice were maintained in the animal facility of Okayama University under specific pathogen-free (SPF) conditions. Mice were housed under a 12-h light/dark cycle with free access to food and water. Male BALB/c and B10.BR. mice (5–16 weeks old) were used for experiments. All animal experiments were conducted in compliance with the ARRIVE guidelines and were approved by the Animal Care and Use Committee of Okayama University (OKU-2023363). All procedures were performed in accordance with the Act on Welfare and Management of Animals of Japan and the Guidelines for Proper Conduct of Animal Experiments issued by the Science Council of Japan, which are in accordance with internationally accepted principles for animal research.

Table 1
Bacterial strains used in this study.

Species	Strain	Genotypes or characteristics	Source or reference
Escherichia coli	BW25113	*rrnB*, Δ*lacZ*4787, *HsdR*514, Δ(*araBAD*)567, Δ(*rhaBAD*)568, *rph-1*	NBRP
Bacillus subtilis	168	*trpC2*	BGSC
Lactococcus lactis	MG1363	Wild-type strain	[14]
Staphylococcus aureus	Newman	Laboratory strain, high level of clumping factor	[15]
	MN1844	Newman Δ*agr*::*tetM* (transduction from RN6911)	[16]
	YS1	Newman Δ*psmα1-4*::*ermAM*	[17]

2.4. Bacterial culture

The *S. aureus* strains (Table 1) were grown in tryptic soy broth (TSB) or on TSB agar plates under aerobic conditions at 37 °C overnight. *E. coli* and *B. subtilis* strains (Table 1) were cultured in LB medium under the same conditions. *Lactococcus lactis* strain (Table 1) was cultured in GM17 medium at 30 °C under aerobic conditions overnight.

2.5. Preparation of heat-killed bacteria

Bacteria grown overnight in liquid medium were washed with PBS and adjusted by optical density at 600 nm. Cultures were autoclaved at 121 °C for 20 min to prepare heat-killed bacteria. Cell numbers were normalized based on OD_{600} values before addition to DC cultures.

2.6. Cell stimulation

DC2.4 cells (5×10^5 cells/well) were seeded in 6-well plates with 1 mL RPMI-1640 medium. Cells were stimulated with live or heat-killed bacteria (MOI = 1–30), or with peptidoglycan, LPS, poly(I:C), or butyrate at the indicated concentrations, and incubated for 24 h at 37 °C in 5% CO_2. When DC2.4 cells were stimulated with live *S. aureus* for 24 h, the cells were first incubated in antibiotic-free RPMI-1640 medium for 1 h, after which gentamicin was added at 50 μg/mL.

2.7. Measurement of dendrite extension

Dendrite extension was quantified as previously described (9). Briefly, DC2.4 cells were stimulated for 24 h, and cell morphology was observed with an inverted phase-contrast microscope (Olympus CKX41). Images were acquired at 200× magnification with a Nikon Digital Sight 1000 camera. Dendrite extension was quantified using ImageJ software. Bright-field images were acquired, and fields of view were randomly selected for analysis to avoid selection bias. Individual cells within each field were analyzed. For each cell, the longest dendritic protrusion extending from the cell body was identified, and its length was manually measured using the line tool in ImageJ (Fig. S7). The measurement was defined as the distance from the edge of the cell body to the tip of the longest protrusion. At least 100 cells were analyzed per experiment, and three independent experiments were performed (>300 cells in total).

2.8. Generation of knockout cells

TLR2-and MyD88-deficient DC2.4 cells were generated using a CRISPR/Cas9-based method as previously described [18]. gRNA sequences targeting TLR2 or MyD88 (Table 2) were cloned into peSpCas9 (1.1)-2×sgRNA (Addgene #80768). This plasmid and pDonor-tBFP-NLS-Neo (Addgene #80767) were transfected into DC2.4 cells using PEI-MAX. Following G418 selection and limiting dilution cloning, knockout clones were isolated. TLR2 deficiency was

Table 2
Oligonucleotide primers used in this study.

Target	Oligonucleotide sequence(5′ to 3′)	Description
ARP2_#1	CACAGATCCCCACCAGAGAAACTCAATATAGACTCGAGTCTATATTGAGTTTCTCTGGTTTTTTAAGCTT	shRNA
ARP2_#2	CACAGATCCCCGTGTTAGTTGAGTCATATACACTCGAGTGTATATGACTCAACTAACAC TTTTTAAGCTT	shRNA
CRMP2_#1	CACAGATCCCCGTCCTTCTATGCAGACATATACTCGAGTATATGTCTGCATAGAAGGACTTTTTAAGCTT	shRNA
CRMP2_#2	CACAGATCCCCATGATCATTGACCATGTTGTTCTCGAGAACAACATGGTCAATGATCATTTTTTAAGCTT	shRNA
ARP2	TGCCATCGAGGTTGGAACGA	RT-PCR
	ATGTCTGCTAGGACTGCGCC	RT-PCR
CRMP2	GACCATGTTGTTCCTGAGCCC	RT-PCR
	GCCATGTACACGAGGAAGGAG	RT-PCR
GAPDH	TGTGTCCGTCGTGGATCTGA	RT-PCR
	TTGCTGTTGAAGTCGCAGGAG	RT-PCR
MyD88	CACCCTTGAACCCTCGGACGCCCG	Knock out
	AAACCGGGCGTCCGAGGGTTCAAG	Knock out
TLR2	CACCGGAGGTTCGCACACGCTCGG	Knock out
	AAACCCGAGCGTGTGCGAACCTCC	Knock out
TLR4	CACCACACGTCCATCGGTTGATCT	Knock out
	AAACAGATCAACCGATGGACGTGT	Knock out
Target	Oligonucleotide sequence(5′ to 3′)	Description
ARP2_#1	CACAGATCCCCACCAGAGAAACTCAATATAGACTCGAGTCTATATTGAGTTTCTCTGGTTTTTTAAGCTT	shRNA
ARP2_#2	CACAGATCCCCGTGTTAGTTGAGTCATATACACTCGAGTGTATATGACTCAACTAACAC TTTTTAAGCTT	shRNA
CRMP2_#1	CACAGATCCCCGTCCTTCTATGCAGACATATACTCGAGTATATGTCTGCATAGAAGGACTTTTTAAGCTT	shRNA
CRMP2_#2	CACAGATCCCCATGATCATTGACCATGTTGTTCTCGAGAACAACATGGTCAATGATCATTTTTTAAGCTT	shRNA
ARP2	TGCCATCGAGGTTGGAACGA	RT-PCR
	ATGTCTGCTAGGACTGCGCC	RT-PCR
CRMP2	GACCATGTTGTTCCTGAGCCC	RT-PCR
	GCCATGTACACGAGGAAGGAG	RT-PCR
GAPDH	TGTGTCCGTCGTGGATCTGA	RT-PCR
	TTGCTGTTGAAGTCGCAGGAG	RT-PCR
MyD88	CACCCTTGAACCCTCGGACGCCCG	Knock out
	AAACCGGGCGTCCGAGGGTTCAAG	Knock out
TLR2	CACCGGAGGTTCGCACACGCTCGG	Knock out
	AAACCCGAGCGTGTGCGAACCTCC	Knock out
TLR4	CACCACACGTCCATCGGTTGATCT	Knock out
	AAACAGATCAACCGATGGACGTGT	Knock out

The underlined sequence indicates the target sequence, and the double-underlined sequence represents the loop sequence for shRNA.

confirmed by flow cytometry (Fig. S1A), and MyD88 deficiency by immunoblotting (Fig. S1B). Two independent clones (KO#1 and KO#2) were used in experiments. For generating TLR4 deficient DC2.4 cells, the gRNA sequence targeting TLR4 (Table 2) was cloned into lentiCPISPR v2 vector (Addgene #52961). Lentiviral particles were produced in HEK293FT cells by transfection together with packaging vectors (pLP1, pLP2, pVSVG (Thermo Fisher Scientific)) using PEI-MAX. DC2.4 cells were transduced with the lentivirus, and knockout clones were isolated following puromycin selection and limiting dilution cloning. TLR4 deficiency was confirmed by immunoblotting (Fig. S3A). The genomic region surrounding the sgRNA target site was amplified by PCR and subjected to sequence analysis to confirm genome editing. Both alleles of TLR4 were found to contain mutations at the predicted cleavage site. These mutations introduced premature stop codons in close proximity to the Cas9 cleavage site, indicating successful biallelic disruption of the TLR4 gene. Sequence alignment was performed using the ClustalW web-based tool (Fig. S3B). To functionally validate TLR4 deficiency, cells were stimulated with LPS or PGN, and cytokine production was assessed. TLR4-knockout cells failed to produce IL-6 in response to LPS stimulation, whereas IL-6 production in response to PGN was preserved, confirming the selective loss of TLR4-dependent signaling (Fig. S3C).

2.9. Generation of knockdown cells

Lentiviral particles were produced in HEK293FT cells by transfection with the FHUG + W(B2) plasmid (Addgene #74011), in which the target sequence (Table 2) was inserted downstream of the H1 promoter to express the shRNAs, together with packaging vectors (pLP1, pLP2, pVSVG using PEI-MAX. DC2.4 cells were transduced with lentiviruses, and knockdown efficiency was confirmed by qPCR (Fig. S4).

2.10. Immunoblot

Immunoblot analyses were performed as described previously [8]. The samples were subjected to SDS-PAGE and transferred to a polyvinylidene difluoride membrane. Anti-pAkt, anti-Akt, anti-pERK, anti--ERK and anti-GAPDH antibodies were used as primary antibodies. HRP-conjugated anti-rabbit IgG, or anti-mouse IgG were used as a secondary antibody. The detected bands were quantified using Image J software.

2.11. Quantitative PCR

Total RNA was extracted from DC2.4 cells using the NucleoSpin RNA kit (Takara Bio). cDNA was synthesized with PrimeScript RT reagent kit (Takara Bio) according to the manufacturer's instructions. Quantitative PCR was performed using a QuantStudio 3 real-time PCR system (Thermo Fisher Scientific). Expression levels were normalized to GAPDH. Primer sequences are listed in Table 2.

2.12. Antigen uptake assay

For soluble antigen uptake, DC2.4 cells were incubated with FITC-OVA (4 μg/mL) for 2 h. Cells were washed with FACS buffer (PBS with 2% FBS) and analyzed by flow cytometry (FACSCalibur; BD Biosciences). For particulate antigen uptake, cells were incubated with FITC-labeled microspheres (2 μL/mL) for 2 h, washed, and bead-positive cells were quantified by flow cytometry.

2.13. Flow cytometry analysis

Cells were harvested and washed with FACS-SM buffer (PBS without Ca^{2+} and Mg^{2+}, supplemented with 2% FBS and 0.05% NaN_3). The cells

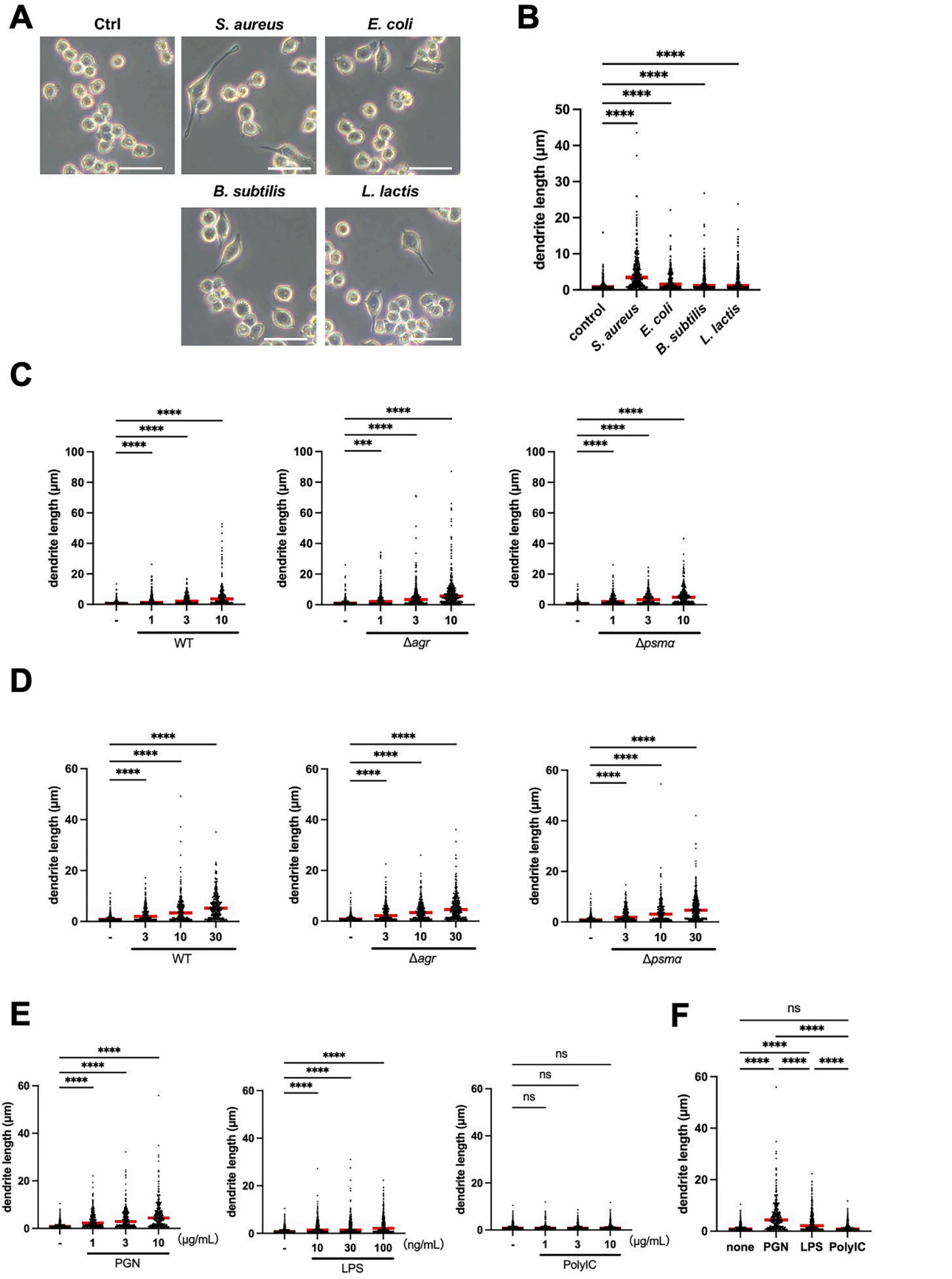

(caption on next page)

Fig. 1. Peptidoglycan from *S. aureus* induces dendrite extension in dendritic cells.
(A) DC2.4 cells were treated with heat-killed *S. aureus*, *E. coli*, *B. subtilis*, or *L. lactis* at an MOI of 30 for 24 h at 37 °C. Cells were observed by phase-contrast microscopy. Scale bar = 50 μm
(B) Quantification of dendrite extension under the conditions shown in (A).
(C) DC2.4 cells were treated with live bacterial cells (MOI = 1, 3, or 10) of wild-type *S. aureus*, Δ*agr*, or Δ*psmα* mutants for 24 h at 37 °C.
(D) DC2.4 cells were treated with heat-killed wild-type, Δ*agr*, or Δ*psmα* mutants (MOI = 3, 10, or 30) for 24 h at 37 °C
(E) DC2.4 cells were stimulated with PGN, LPS, or poly(I:C).
(F) Comparison of dendrite extension following treatment with PGN (10 μg/mL), LPS (100 ng/mL), or poly(I:C) (10 μg/mL).
For each experiment, the length of the longest dendrite from each cell body was measured. Each dot represents an individual cell; thick red horizontal lines indicate the mean. At least 100 cells were analyzed per experiment, and data represent ≥300 cells pooled from three independent experiments. Statistical significance was determined by Dunnett's (B-E) or Tukey's (F) multiple comparison tests. *$p < 0.05$, **$p < 0.01$, ***$p < 0.001$, ****$p < 0.0001$; ns indicates no significant difference. (For interpretation of the references to colour in this figure legend, the reader is referred to the Web version of this article.)

were then incubated with fluorochrome-conjugated antibodies in FACS-SM on ice for 30 min. After three washes, the samples were analyzed using a flow cytometer (Gallios; Beckman Coulter).

2.14. Mixed lymphocyte reaction

An MLR assay was performed following a previously described protocol [19,20]. Lymph nodes were harvested from BALB/c mice, mechanically disrupted, and filtered through 40-μm strainers to obtain single-cell suspensions. DC2.4 cells were stimulated with heat-killed *S. aureus* and/or butyrate for 24 h. After stimulation, cells were extensively washed to remove residual stimuli. Specifically, cells were washed at least three times with fresh culture medium and resuspended in stimulus-free medium prior to co-culture. Washed DCs were then co-cultured with lymph node cells at a 1:5 ratio for 72 h. Culture supernatants were collected and IL-10, IL-17, and IFN-γ concentrations were measured by ELISA. Naïve $CD4^+$ T cells were isolated from mouse splenocytes using a magnetic bead–based isolation kit (BioLegend), according to the manufacturer's instructions. Briefly, cells were incubated with a cocktail of biotin-labeled antibodies and streptavidin-conjugated magnetic beads, and naïve $CD4^+$ T cells were purified by negative selection using a magnetic separation system.

2.15. Statistical analyses

All statistical analyses were performed using Prism software (v10.5.0). The statistical tests used for each dataset are described in the corresponding figure legends.

3. Results

3.1. Peptidoglycan from S. aureus induces dendrite extension in dendritic cells

In the intestinal environment, DCs are constantly exposed to diverse bacterial species. However, it remains unclear whether bacterial stimulation directly influences DC morphology. To address this, we first examined the effects of several bacterial species—including *S. aureus*, *Bacillus subtilis*, *Lactococcus lactis*, and *Escherichia coli*—on dendrite formation. Each bacterium was added to DC2.4 cells at a multiplicity of infection (MOI) of 30, and morphological changes were assessed. All tested bacteria induced dendrite extension to varying degrees, with *S. aureus* showing the most pronounced effect (Fig. 1A and B).

Next, DC2.4 cells were stimulated with increasing doses of *S. aureus* (MOI = 1, 3, or 10). After 24 h, dendrite extension was observed in a dose-dependent manner (Fig. 1C). To investigate whether known virulence regulators contribute to this phenotype, we examined mutants lacking the *agr* locus, a positive regulator of toxin production, or its downstream effector PSMα. Both mutants retained the same dendrite-extending activity as the wild-type strain (Fig. 1C).

We then assessed whether heat-sensitive factors such as secreted toxins were required for this effect. Heat-killed *S. aureus* induced dendrite extension to a similar extent as live bacteria (Fig. 1D), suggesting that stable bacterial cell wall components may be responsible. Because PGN is a major cell wall component of *S. aureus* and a known ligand for innate immune receptors, we hypothesized that PGN mediates dendrite extension. To test this, DC2.4 cells were stimulated with purified PGN, lipopolysaccharide (LPS), or poly(I:C). PGN stimulation strongly induced dendrite extension, whereas LPS induced weaker responses and poly(I:C) had no detectable effect (Fig. 1E). Comparative analysis confirmed that PGN exerted a significantly stronger effect than LPS (Fig. 1F). Taken together, these findings indicate that *S. aureus* peptidoglycan is a key factor driving dendrite extension in DCs.

3.2. Dendrite extension induced by S. aureus requires the TLR2 signaling pathway

Based on our observation that PGN triggered dendrite extension, we next investigated the role of its cognate receptor, Toll-like receptor 2 (TLR2) [21,22]. Using CRISPR/Cas9 genome editing, we generated DC2.4 cell lines deficient in TLR2, TLR4 or their adaptor protein MyD88 (Fig. S1–S2). When stimulated with *S. aureus*, both TLR2-and MyD88--deficient cells failed to extend dendrites, in contrast to wild-type DC2.4 cells (Fig. 2A–C, S3), whereas TLR4-deficient cells retained the ability to undergo dendrite extension (Fig. 2A and D). To determine whether this requirement was specific to *S. aureus*–mediated signaling, we stimulated the same knockout cell lines with butyrate, a representative SCFA. In this case, dendrite extension was comparable between wild-type, TLR2-, TLR4-and MyD88-deficient DC2.4 cells (Fig. 2A–D). These findings demonstrate that dendrite extension induced by *S. aureus* depends on TLR2/MyD88 signaling, whereas SCFA-mediated dendrite extension occurs independently of this pathway.

3.3. S. aureus–induced dendrite extension is mediated by the ERK signaling pathway

TLR2 signaling is known to activate several downstream pathways, including MAPK cascades (ERK, JNK, and p38) as well as the NF-κB pathway *via* IKK [23–26]. To determine which signaling pathway mediates dendrite extension, we treated DC2.4 cells with specific pharmacological inhibitors. Inhibition of MEK, the upstream activator of ERK, by U0126, or PD98059 markedly suppressed dendrite extension induced by *S. aureus* (Fig. 3A and B). Treatment with U0126 did not affect cell viability under the experimental conditions, as confirmed by viability assays (Fig. S4). By contrast, inhibition of JNK, p38, or IKK had little or no effect on dendrite extension (Fig. 3B–D). These results indicate that *S. aureus* peptidoglycan promotes dendrite extension primarily through TLR2/MyD88-dependent activation of the ERK pathway. Given that pharmacological inhibition of the ERK pathway suppressed dendrite extension, we next examined whether *S. aureus* stimulation activates ERK signaling. Immunoblot analysis revealed that *S. aureus* stimulation markedly increased ERK phosphorylation compared to unstimulated controls, indicating activation of the ERK signaling pathway (Fig. 3F).

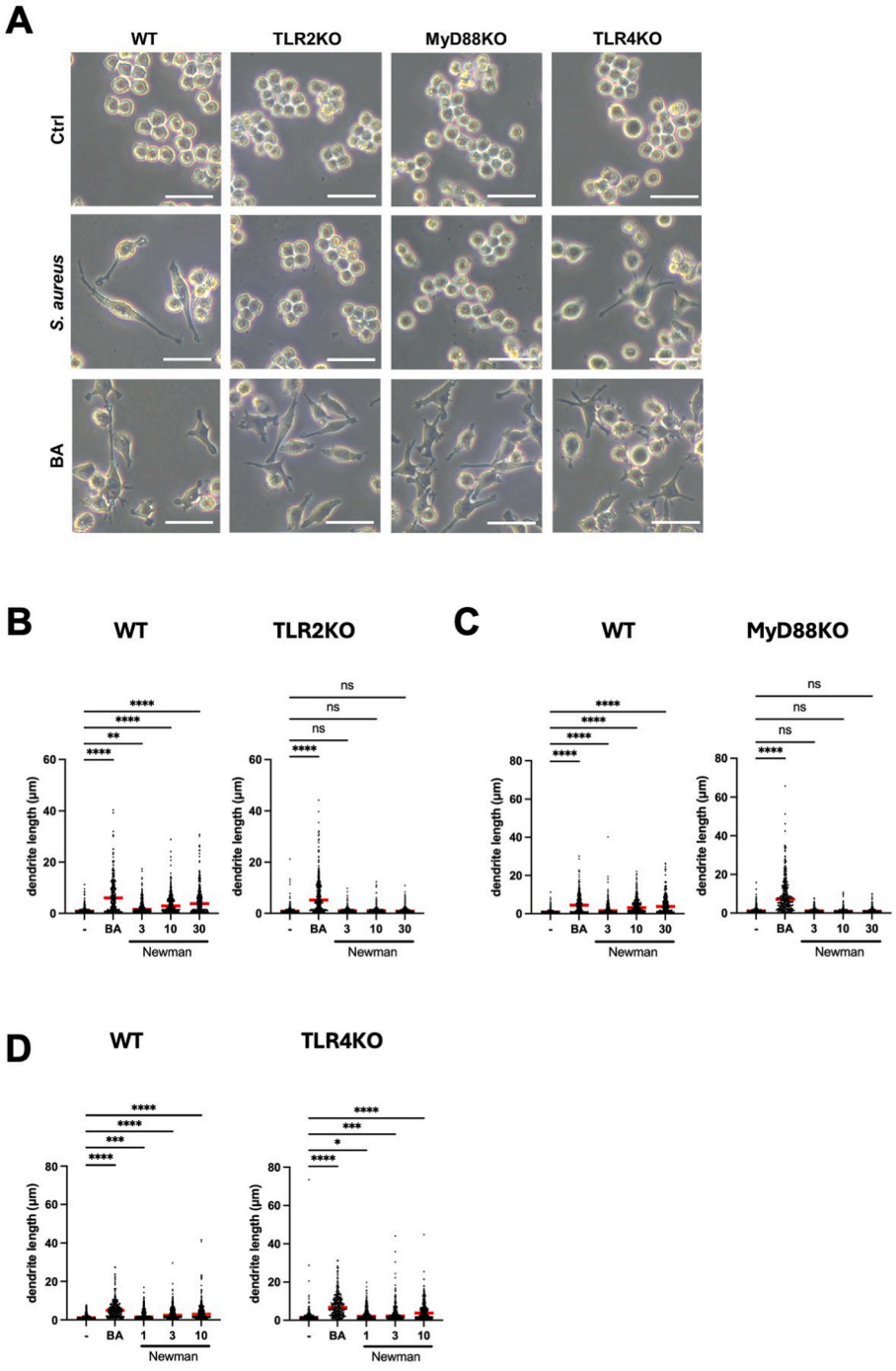

Fig. 2. Dendrite extension induced by *S. aureus* requires the TLR2 signaling pathway.
(A) Wild-type DC2.4 cells, TLR2-deficient cells, and MyD88-deficient cells were stimulated with butyrate (1 mM) or heat-killed *S. aureus* (MOI = 30) and incubated for 24 h. Cells were observed by phase-contrast microscopy. Representative images from three independent experiments are shown. Scale bar = 50 μm
(B, C, D) Wild-type DC2.4 cells, TLR2-deficient cells, and MyD88-deficient cells were stimulated with butyrate (1 mM) or heat-killed *S. aureus* (MOI = 3, 10, or 30) and incubated for 24 h. The dendrite extensions were quantified. The length of the longest dendrite from each cell body was measured. Each dot represents an individual cell; thick red horizontal lines indicate the mean. At least 100 cells were analyzed per experiment, and data represent ≥300 cells pooled from three independent experiments. Statistical significance was determined by Dunnett's multiple comparison test. *$p < 0.05$, **$p < 0.01$, ***$p < 0.001$, ****$p < 0.0001$. ns indicates no significant difference. (For interpretation of the references to colour in this figure legend, the reader is referred to the Web version of this article.)

3.4. Actin polymerization is required for dendrite extension induced by S. aureus

Cytoskeletal remodeling is generally essential for morphological changes in cells. We previously demonstrated that SCFA-induced dendrite extension depends on PI3K-mediated activation of the Rho family GTPase Cdc42, which promotes actin polymerization [8]. To examine whether *S. aureus*–induced dendrite extension involves similar mechanisms, we first treated DC2.4 cells with cytochalasin B, an inhibitor of actin polymerization. Cytochalasin B effectively suppressed dendrite extension, indicating a requirement for actin remodeling (Fig. 4A).

We next tested the contribution of specific Rho family GTPases. Inhibition of Cdc42 with ML141 strongly reduced dendrite extension

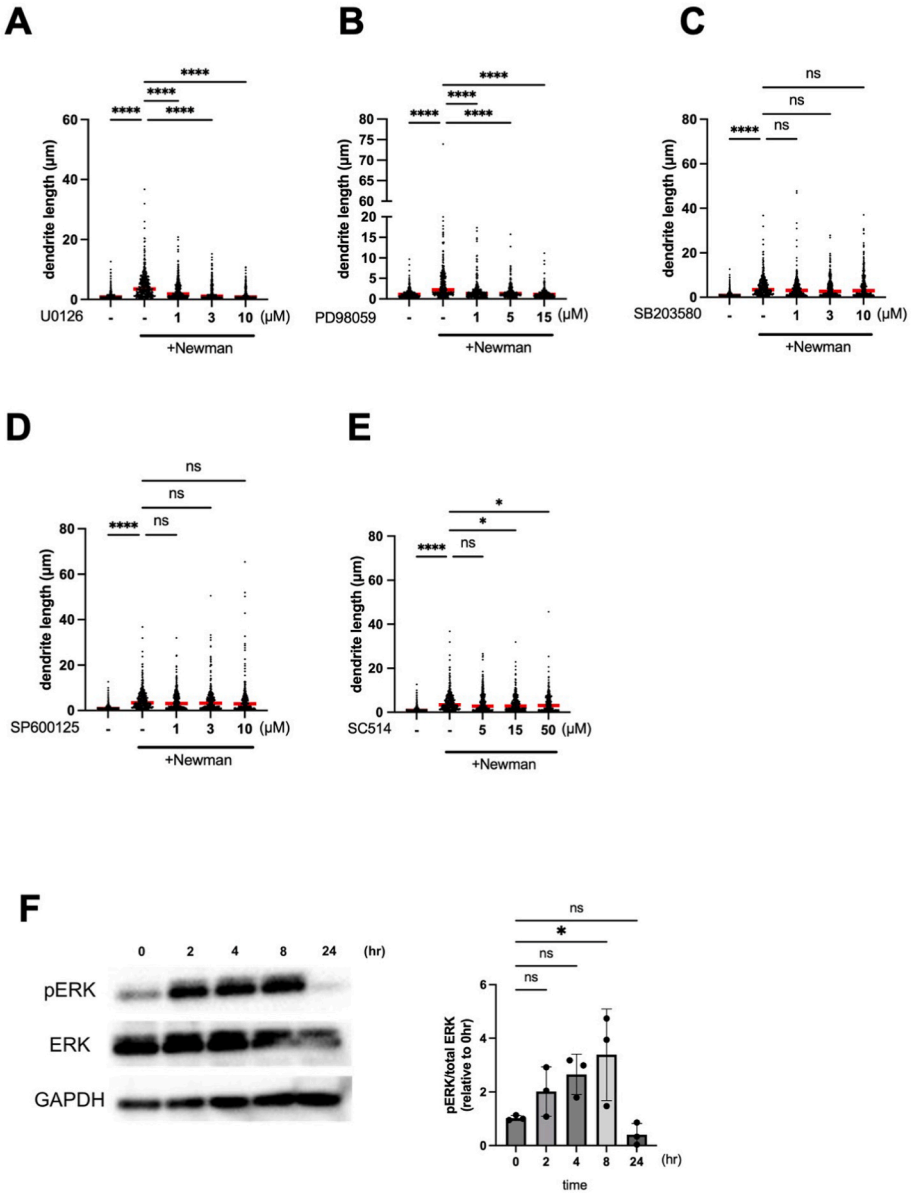

Fig. 3. Dendrite extension induced by *S. aureus* is mediated by the ERK signaling pathway.
DC2.4 cells were stimulated with heat-killed *S. aureus* (MOI = 30) in the presence of inhibitors and incubated for 24 h. (A) Effect of the MEK inhibitor U0126 (1, 3, 10 μM). (B) Effect of the MEK inhibitor PD98059 (1, 3, 10 μM). (C) Effect of the p38 MAPK inhibitor SB203580 (1, 3, 10 μM). (D) Effect of the JNK inhibitor SP600125 (1, 3, 10 μM). (E) Effect of the IKK inhibitor SC514 (5, 15, 50 μM). The length of the longest dendrite from each cell body was measured. Each dot represents an individual cell; thick red horizontal lines indicate the mean. At least 100 cells were analyzed per experiment, and data represent ≥300 cells pooled from three independent experiments.
(F) DC2.4 cells were incubated with heat-killed *S. aureus* (MOI = 30) for 0, 2, 4, 8, and 24 h. The cells were harvested and the amounts of pERK, ERK, and GAPDH were detected using immunoblotting with specific antibodies. Right graphs indicate quantification of bands. Values are averages ± SD (n = 3). Statistical significance was determined by Dunnett's multiple comparison test. *p < 0.05, **p < 0.01, ***p < 0.001, ****p < 0.0001. ns indicates no significant difference. (For interpretation of the references to colour in this figure legend, the reader is referred to the Web version of this article.)

(Fig. 4B), whereas inhibition of Rac1 with EHT1864 had little effect (Fig. 4C). Inhibition of Rho-associated kinase (ROCK), a downstream effector of RhoA, by Y27632 even enhanced dendrite extension (Fig. 4D). Because PI3K signaling can act upstream of Cdc42 and Rac1, we also examined the effect of the PI3K inhibitor LY294002. This treatment suppressed *S. aureus*–induced dendrite extension (Fig. 4E). Together, these results indicate that *S. aureus* induces dendrite extension in DC2.4 cells through PI3K-dependent activation of Cdc42 and subsequent actin cytoskeletal remodeling.

3.5. Arp2 and CRMP2 contribute to dendrite extension induced by *S. aureus*

Cytoskeletal dynamics involving both actin and microtubules play crucial roles in cellular morphological changes. Arp2 functions as a nucleation factor within the Arp2/3 complex to initiate branched actin filament assembly [27–29], whereas CRMP2 regulates microtubule polymerization downstream of GSK3β and is essential for axonal extension and guidance in neurons [30,31]. To examine whether these molecules also contribute to dendrite extension in DCs, we analyzed the roles of Arp2 and CRMP2. Treatment with CK666, an inhibitor of the Arp2/3 complex, suppressed dendrite extension in a dose-dependent

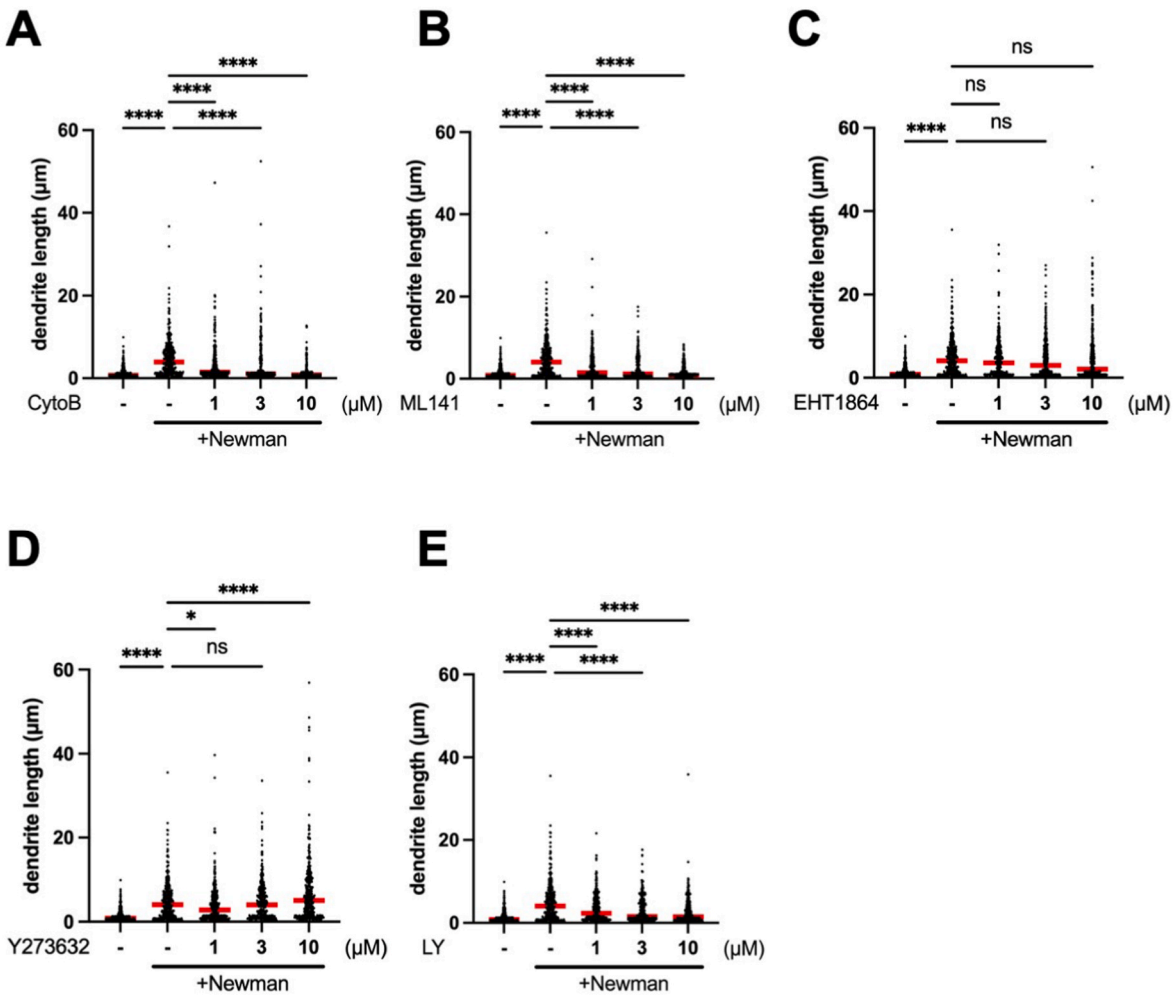

Fig. 4. Actin polymerization is required for dendrite extension induced by *S. aureus*.
(A–E) DC2.4 cells were stimulated with heat-killed *S. aureus* (MOI = 30) in the presence of cytochalasin B (CytoB; 1, 3, 10 μM), ML141 (1, 3, 10 μM), EHT1864 (1, 3, 10 μM), Y27632 (1, 3, 10 μM), or LY294002 (1, 3, 10 μM), and incubated for 24 h. Dendrite length was quantified as described in Fig. 1. At least 100 cells were analyzed per experiment, and data represent ≥300 cells pooled from three independent experiments. Statistical significance was determined by Dunnett's multiple comparison test. *$p < 0.05$, **$p < 0.01$, ***$p < 0.001$, ****$p < 0.0001$. ns indicates no significant difference.

manner (Fig. 5A). Consistently, knockdown of Arp2 by shRNA reduced dendrite formation (Fig. S3A; Fig. 5B and C). Similarly, inhibition of GSK3β with CHIR99021, which activates CRMP2, enhanced dendrite extension at 1–3 μM but markedly inhibited it at 10 μM (Fig. 5A). Furthermore, shRNA-mediated knockdown of CRMP2 also suppressed dendrite extension (Fig. S5B; Fig. 5B and D). These findings suggest that *S. aureus*–induced dendrite extension requires both branched actin network formation *via* Arp2 and microtubule polymerization controlled by CRMP2.

3.6. *S. aureus* and SCFA stimulation synergistically promote dendrite extension

We previously demonstrated that short- SCFAs induce dendrite extension in DCs [8]. To determine whether *S. aureus* and SCFAs act through independent pathways, we compared the effects of single versus combined stimulation. DC2.4 cells were treated with *S. aureus*, butyrate, or both, and dendrite morphology was assessed. Whereas either stimulus alone promoted dendrite extension, co-stimulation with *S. aureus* and butyrate resulted in a significantly greater degree of dendrite extension compared with either treatment alone (Fig. 6A and B). These results indicate that *S. aureus* and SCFAs act additively through distinct mechanisms to enhance dendrite extension in DCs.

We next examined whether co-stimulation with *S. aureus* and butyrate affects Akt activation. Immunoblot analysis revealed that while *S. aureus* alone induced Akt phosphorylation, co-stimulation with BA further enhanced Akt phosphorylation compared to stimulation with *S. aureus* alone. These results indicate that BA potentiates *S. aureus*-induced Akt signaling (Fig. 6C).

To determine whether the observed effects are reproducible in primary dendritic cells, we examined dendrite extension in bone marrow–derived dendritic cells (BMDCs). Stimulation with *S. aureus* induced clear dendrite extension in BMDCs (Fig. 6D). Importantly, co-stimulation with *S. aureus* and butyrate resulted in a markedly greater elongation of dendrites compared to either stimulus alone (Fig. 6E and F). This enhanced response was consistent with the synergistic effect observed in DC2.4 cells.

3.7. Functional consequences of dendrite extension induced by *S. aureus*

SCFA stimulation not only promotes dendrite extension but also enhances antigen uptake and presentation by DCs [8]. To examine whether *S. aureus*–induced dendrite extension confers similar functional advantages, we compared the effects of *S. aureus*, butyrate, or their combination on antigen uptake. Using fluorescein isothiocyanate (FITC)–labeled ovalbumin (OVA) as a model soluble antigen and

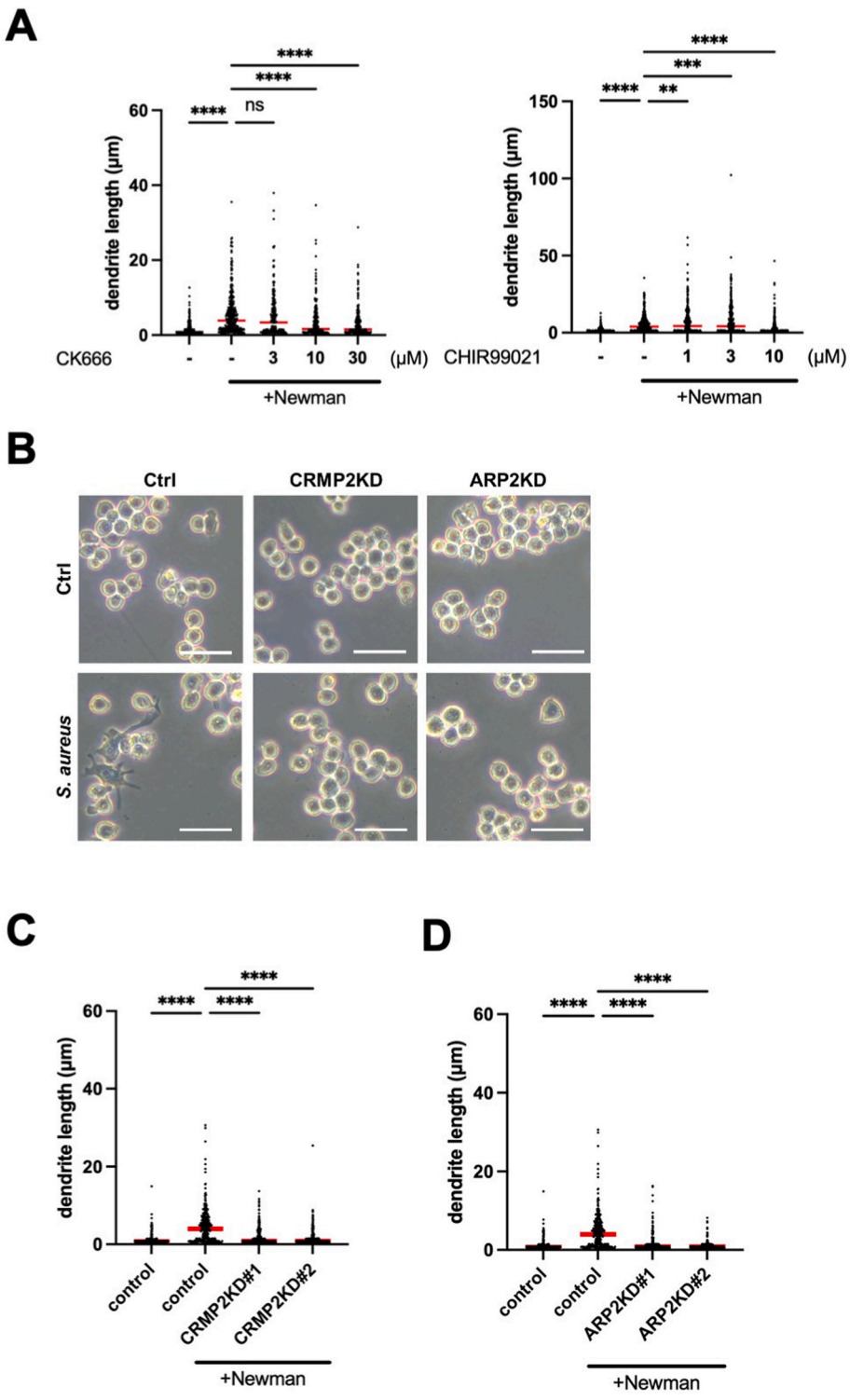

Fig. 5. Arp2 and CRMP2 contribute to dendrite extension induced by *S. aureus*.
(A) DC2.4 cells were stimulated with heat-killed *S. aureus* (MOI = 30) in the presence of CHIR99021 (1, 3, 10 μM) or CK666 (3, 10, 30 μM), and incubated for 24 h (B) Control DC2.4 cells, CRMP2 knockdown (CRMP2 KD) cells, and Arp2 knockdown (Arp2 KD) cells were stimulated with heat-killed *S. aureus* (MOI = 30) and incubated for 24 h. Cells were observed by phase-contrast microscopy. Representative images from three independent experiments are shown. Scale bar = 50 μm (C, D) Quantification of dendrite extension under the conditions shown in (B). (B) Comparison of Control DC2.4 cells versus CRMP2 knockdown (CRMP2 KD) cells. (C) Comparison of Control DC2.4 cells versus Arp2 knockdown (Arp2 KD) cells.
Dendrite length was measured as described in Fig. 1. At least 100 cells were analyzed per experiment, and data represent ≥300 cells pooled from three independent experiments. Statistical significance was determined by Dunnett's multiple comparison test. *$p < 0.05$, **$p < 0.01$, ***$p < 0.001$, ****$p < 0.0001$. ns indicates no significant difference.

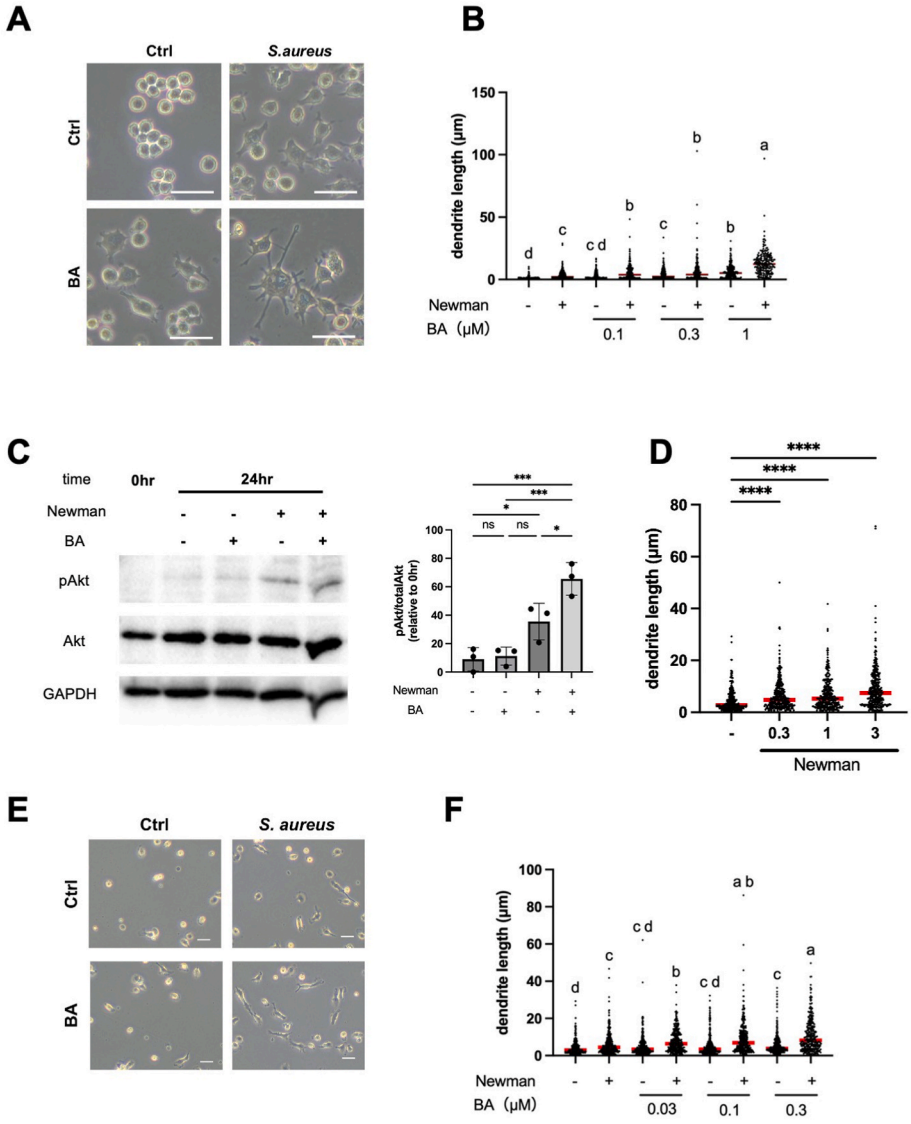

Fig. 6. Co-stimulation with *S. aureus* and SCFAs synergistically promotes dendrite extension.
(A) DC2.4 cells were stimulated with butyrate (1 mM) and heat-killed *S. aureus* (MOI = 30) and incubated for 24 h. Cells were observed by phase-contrast microscopy. Representative images from three independent experiments are shown. Scale bar = 50 μm
(B) DC2.4 cells were stimulated with butyrate (0.1, 0.3, or 1 mM) in combination with heat-killed *S. aureus* (MOI = 30) for 24 h, and dendrite extension was quantified. Dendrite length was measured as described in Fig. 1. At least 100 cells were analyzed per experiment, and data represent ≥300 cells pooled from three independent experiments.
(C) DC2.4 cells were incubated with butyrate (1 mM) and heat-killed *S. aureus* (MOI = 30) for 24 h. The cells were harvested and the amounts of pAkt, Akt, and GAPDH were detected using immunoblotting with specific antibodies. Right graphs indicate quantification of bands. Values are averages ± SD (n = 3).
(D) BMDCs cells were stimulated with heat-killed *S. aureus* (MOI = 0, 0.3, 1, 3) and incubated for 24 h. Cells were observed by phase-contrast microscopy. Dendrite length was measured as described in Fig. 1. At least 100 cells were analyzed per experiment, and data represent ≥300 cells pooled from three independent experiments.
(E, F) BMDCs cells were stimulated with butyrate (0.3 mM) and heat-killed *S. aureus* (MOI = 1) and incubated for 24 h. Cells were observed by phase-contrast microscopy. Representative images from three independent experiments are shown. Scale bar = 50 μm.
For each experiment, the length of the longest dendrite from each cell body was measured. Each dot represents an individual cell; thick red horizontal lines indicate the mean. At least 100 cells were analyzed per experiment, and data represent ≥300 cells pooled from three independent experiments. Statistical significance was determined by Tukey's multiple comparison test (B, F). Different letters indicate statistically significant differences among groups ($p < 0.05$). Statistical significance was determined by Dunnett's multiple comparison test (C, D). *$p < 0.05$, **$p < 0.01$, ***$p < 0.001$, ****$p < 0.0001$. (For interpretation of the references to colour in this figure legend, the reader is referred to the Web version of this article.)

fluorescent beads as an insoluble antigen, we found that stimulation with *S. aureus* increased uptake of both types of antigens (Fig. 7A and B). Notably, co-stimulation with *S. aureus* and butyrate further enhanced bead uptake compared with *S. aureus* alone, whereas uptake of soluble FITC–OVA was not significantly different between the single and combined stimulations (Fig. 7A and B). These results suggest that *S. aureus* and SCFAs cooperatively augment dendrite extension and selectively enhance the phagocytosis of insoluble antigens in DCs.

We examined the effects of *S. aureus* and butyrate on bead uptake in BMDCs. BMDCs stimulated with *S. aureus* exhibited increased bead uptake, whereas BA alone had a limited effect. Importantly, co-stimulation with *S. aureus* and butyrate significantly enhanced uptake compared to either stimulus alone, mirroring the results observed in DC2.4 cells and suggesting a cooperative effect on antigen uptake in primary dendritic

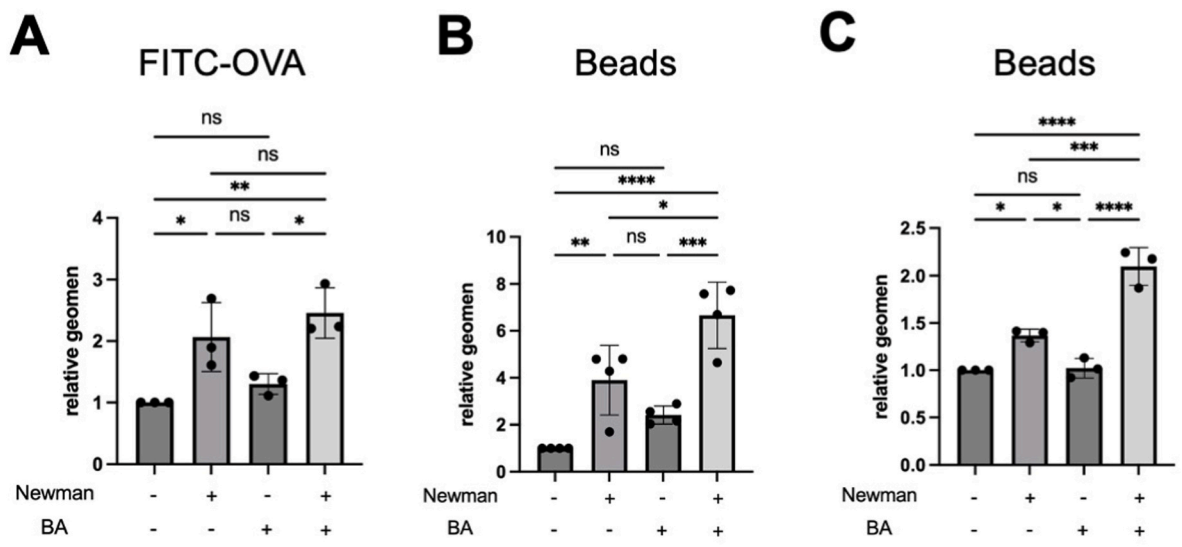

Fig. 7. Functional analysis of dendrite extension induced by *S. aureus*.
(A) DC2.4 cells were stimulated with butyrate (300 μM) and heat-killed *S. aureus* (MOI = 30) for 24 h at 37 °C, then incubated with FITC-labeled OVA for 2 h. Fluorescence intensity was quantified by flow cytometry. Values represent mean ± SD (n = 3).
(B) DC2.4 cells were stimulated with butyrate (300 μM) and heat-killed *S. aureus* (MOI = 30) for 24 h at 37 °C, then incubated with fluorescent beads for 2 h. The proportion of bead-positive cells was measured by flow cytometry. Values represent mean ± SD (n = 4).
(C) BMDCs were stimulated with butyrate (300 μM) and heat-killed *S. aureus* (MOI = 30) for 24 h at 37 °C, then incubated with fluorescent beads for 2 h. The proportion of bead-positive cells was measured by flow cytometry. Values represent mean ± SD (n = 3).
Statistical significance was determined by Tukey's multiple comparison test. *p < 0.05, **p < 0.01, ***p < 0.001, ****p < 0.0001. ns indicates no significant difference.

cells (Fig. 7C).

3.8. Effects of S. aureus and butyrate stimulation on antigen presentation–related molecules

To further evaluate how *S. aureus* and butyrate influence DC antigen presentation, we examined the expression of surface molecules associated with antigen presentation and costimulation. Stimulation with butyrate alone did not induce significant changes in the expression of MHC or costimulatory molecules (Fig. 8A–F). In contrast, *S. aureus* stimulation reduced MHC class I expression (Fig. 8A) and markedly upregulated PD-L1, CD80, and CD86 expression (Fig. 8B, D, 8E). Importantly, co-stimulation with *S. aureus* and butyrate further enhanced the expression of CD40 and CD80 compared with either stimulus alone (Fig. 8D and F). These findings indicate that *S. aureus* and butyrate act cooperatively to enhance the expression of costimulatory molecules, thereby potentially augmenting DC–T cell interactions.

3.9. S. aureus and butyrate co-stimulation enhances differentiation of IL-10– and IL-17–producing T cells

Finally, we assessed how *S. aureus* and butyrate stimulation of DCs influences T cell differentiation using mixed lymphocyte reactions. DC2.4 cells were pretreated with *S. aureus*, butyrate, or both, and then co-cultured with naïve T cells from mouse lymph nodes. Cytokine production was subsequently measured. Stimulation of DCs with either *S. aureus* or butyrate alone did not significantly alter T cell cytokine production compared with unstimulated controls; levels of IL-10, IL-17, and IFN-γ remained low (Fig. 9A–C). In striking contrast, co-stimulation of DCs with *S. aureus* and butyrate led to a marked increase in IL-10 and IL-17 secretion by T cells, whereas IFN-γ remained unchanged (Fig. 9A, B, 9C). These results demonstrate that *S. aureus* and butyrate cooperatively promote DC-mediated differentiation of T cells toward IL-10– and IL-17–producing subsets.Using purified naïve T cells, we observed that co-culture with stimulated dendritic cells induced both IL-10 and IL-17 production, although the levels were lower than those observed with bulk T cells (Fig. S6).

4. Discussion

In this study, we demonstrated that stimulation with *S. aureus* induces dendrite extension in DCs. This morphological change was mediated by recognition of PGN through TLR2, activation of ERK/PI3K signaling, and subsequent Cdc42-dependent actin polymerization. Moreover, *S. aureus* cooperated with the SCFA butyrate to further enhance dendrite extension, antigen uptake, and T cell activation (Fig. 10).

Heat-killed bacteria and purified PGN were sufficient to induce dendrite extension, whereas *S. aureus* mutants lacking the *agr* locus or PSMα exhibited activity comparable to the wild type. These findings suggest that PGN is the principal factor responsible for dendrite extension, rather than protein toxins or secreted virulence factors. Although other Gram-positive bacteria such as *B. subtilis* and *L. lactis* also induced dendrite extension, their effects were weaker than those of *S. aureus*. Differences in PGN structure or modifications [32–35], or the presence of inhibitory components in these bacteria, may explain this variation.

Our inhibitor analyses revealed that dendrite extension by *S. aureus* depends on PI3K-mediated activation of Cdc42, similar to SCFA-induced dendrite extension [8]. This indicates that both stimuli converge on PI3K–Cdc42 signaling to promote actin remodeling. In addition, we identified roles for Arp2 in branched actin filament nucleation and CRMP2 in microtubule polymerization, suggesting that coordinated regulation of both actin and microtubules underlies the dendrite extension by *S. aureus*.

Interestingly, while *S. aureus*–induced dendrite extension was abolished in TLR2-or MyD88-deficient cells, SCFA-induced extension remained intact, indicating that the two pathways operate independently: SCFAs act primarily through HDAC inhibition [8], whereas *S. aureus* acts through TLR2/MyD88/ERK signaling. Importantly, co-stimulation with *S. aureus* and butyrate additively enhanced dendrite extension, antigen uptake, and the expression of costimulatory molecules such as CD40 and CD80. Functional assays further showed that

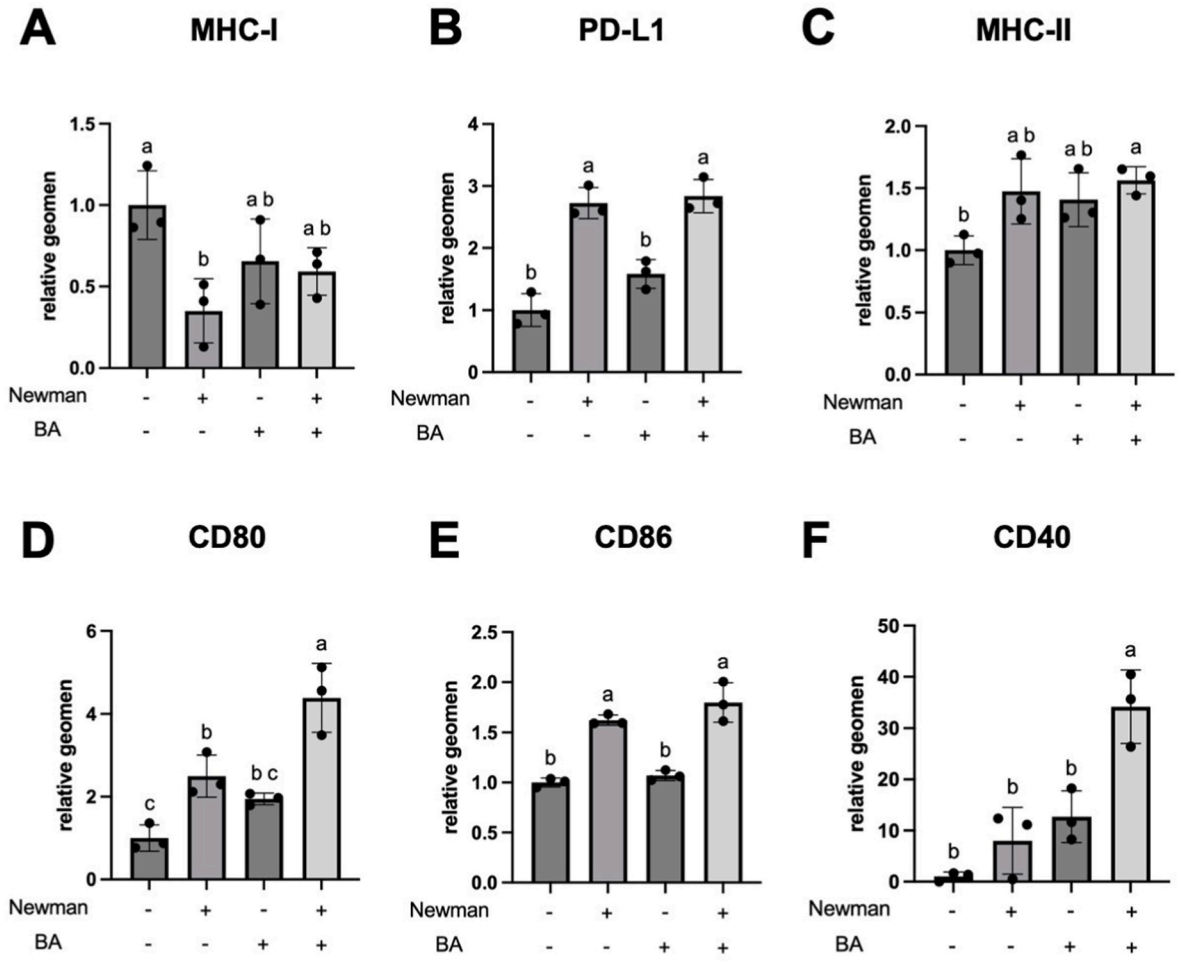

Fig. 8. Effects of *S. aureus* and butyrate stimulation on the expression of antigen presentation–related molecules.
(A–F) DC2.4 cells were stimulated with butyrate (1 mM) and heat-killed *S. aureus* (MOI = 30) for 24 h at 37 °C. Cell surface expression of MHC-I, PD-L1, MHC-II, CD80, CD86, and CD40 was analyzed by flow cytometry. Graphs represent relative mean fluorescence intensity (MFI), normalized to unstimulated cells (set as 1). Values represent mean ± SD (n = 3). Statistical significance was determined by Tukey's multiple comparison test. Different letters indicate statistically significant differences among groups ($p < 0.05$).

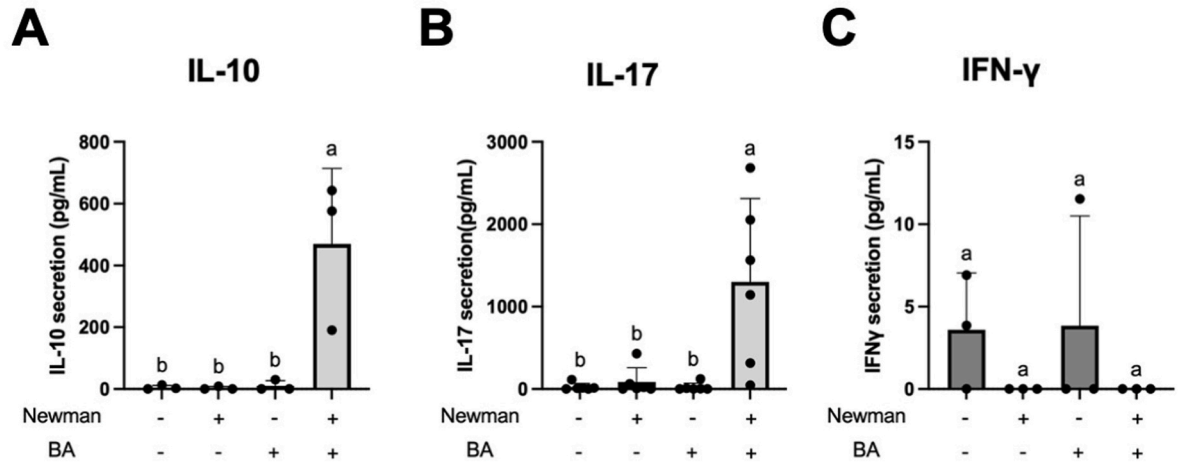

Fig. 9. Effects of *S. aureus* and butyrate co-stimulation on T cell differentiation.
DC2.4 cells were stimulated with heat-killed *S. aureus* (MOI = 30) and butyrate (1 mM) for 24 h at 37 °C. Stimulated DC2.4 cells were co-cultured with lymph node (LN) cells at a DC:LN ratio of 1:5 for 72 h at 37 °C in a mixed lymphocyte reaction (MLR) assay. Concentrations of IL-10, IL-17, and IFN-γ in the culture supernatants were measured by ELISA. Values represent mean ± SD (n ≥ 3). Statistical significance was determined by Tukey's multiple comparison test. Different letters indicate statistically significant differences among groups ($p < 0.05$).

such co-stimulation promoted T cell differentiation toward IL-17– and IL-10–producing subsets, highlighting a cooperative effect of bacterial

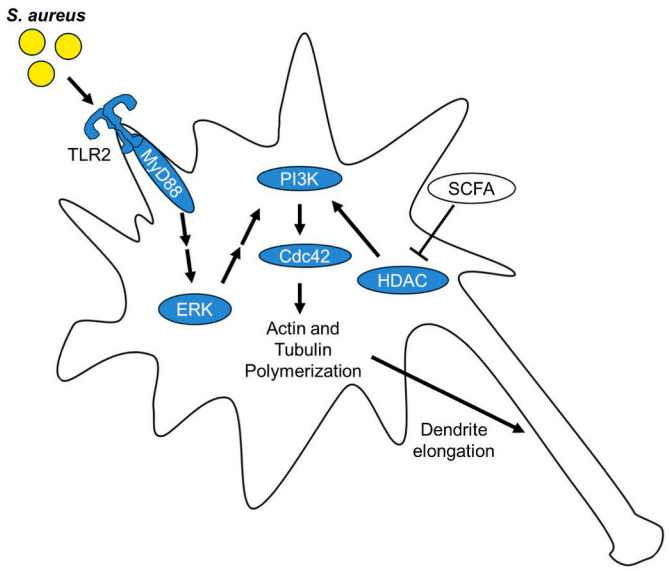

Fig. 10. Schematic model of dendrite elongation in dendritic cells induced by *S. aureus*.
S. aureus stimulates TLR2, leading to ERK activation, which in turn activates Akt/Cdc42 signaling. This activation induces the reorganization of the actin cytoskeleton and microtubules, resulting in dendrite elongation. SCFAs promote Akt/Cdc42 activation through the inhibition of HDACs.

PGN and microbial metabolites on DC activation and T cell polarization.

Although dendritic cell maturation has classically been associated with reduced antigen uptake [36], this concept primarily derives from studies of constitutive fluid-phase uptake and macropinocytosis in immature DCs [37]. More recent work has shown that this is not a universal rule: TLR stimulation can transiently enhance antigen capture through actin remodeling [38] [39], and mature DCs can continue to internalize antigens efficiently through receptor-mediated endocytosis and phagocytosis [40]. Mechanistically, these uptake processes are supported by actin-dependent membrane dynamics and are not uniformly suppressed during maturation [41]. Thus, the increased bead uptake observed here does not necessarily represent a contradiction. One possible explanation is that elongated dendrites increase the effective surface area for particle encounter, thereby enhancing the probability of antigen capture. In addition, the combination of TLR2 signaling and SCFAs may selectively preserve or upregulate specific uptake pathways, such as scavenger receptor–mediated endocytosis or phagocytic receptor activity, which are not uniformly suppressed during DC maturation.

Recent studies have demonstrated that CX3CR1^{+} mononuclear phagocytes in the intestinal mucosa extend transepithelial dendrites to sample luminal antigens. These cells are now considered macrophage-like rather than conventional dendritic cells, and their protrusion is regulated by metabolic cues such as lactate and pyruvate via GPR31 signaling [42]. This process represents a highly specialized mechanism adapted to the intestinal epithelial barrier under homeostatic conditions. In contrast, intestinal DCs are highly motile and actively patrol between epithelial cells, dynamically sampling luminal antigens while migrating within the tissue microenvironment [43]. In this context, the dendrite extension induced by *S. aureus* and SCFAs observed in our study may represent a mechanism that enhances the efficiency of antigen surveillance by mobile DCs. Rather than forming fixed transepithelial protrusions, DCs may utilize dynamic dendritic processes to increase their effective surface area and probability of antigen encounter during migration.

High concentrations of SCFAs are present in the intestinal lumen [44], where *S. aureus* can cause food poisoning and opportunistic infections in immunocompromised hosts [45–47]. Our findings suggest that in the gut, co-stimulation by *S. aureus* and SCFAs may promote dendrite extension, augment antigen uptake, and enhance IL-17 and IL-10 responses, thereby facilitating rapid and effective host defense. We propose that PGN-driven TLR2 signaling not only activates canonical innate immune responses but also triggers dendritic cell morphological changes that optimize antigen sampling and presentation. IL-17 is known to promote antimicrobial defense and barrier integrity [48], whereas IL-10 plays a critical role in limiting excessive inflammation and preventing tissue damage [49]. The simultaneous induction of these cytokines indicates the generation of a functionally balanced T cell response that is both protective and self-limiting. Future studies should determine whether DCs in the gut or nasal mucosa extend dendrites *in vivo* in response to *S. aureus*, and whether additional microbial or host-derived factors regulate dendrite extension. Together, our work identifies PGN recognition by TLR2 as a novel mechanism by which *S. aureus* enhances dendrite extension, working cooperatively with SCFAs to fine-tune DC morphology and function for effgs1:icient immune activation.

CRediT authorship contribution statement

Kai Kobata: Conceptualization, Investigation, Writing – original draft. **Kazuyuki Furuta:** Conceptualization, Funding acquisition, Investigation, Supervision, Writing – original draft. **Yuki Ikeya:** Investigation. **Yohei Chishaki:** Investigation. **Kazuya Ishikawa:** Conceptualization, Funding acquisition, Writing – review & editing. **Chikara Kaito:** Conceptualization, Funding acquisition, Supervision, Writing – original draft.

Declaration of competing interest

The authors declare that they have no known competing financial interests or personal relationships that could have appeared to influence the work reported in this paper.

Acknowledgments

The authors thank Advanced Science Research Center Department of Genomics and Proteomics, Okayama University for providing access to analytical instruments and technical assistance. This study was supported in part by grants from the JSPS KAKENHI (Grant numbers 23K06130 (KF), 24K01760 (KI), 23K24131 (CK)) and Smoking Research Foundation (KF).

Appendix A. Supplementary data

Supplementary data to this article can be found online at https://doi.org/10.1016/j.bbrc.2026.154001.

References

[1] N. Halliday, C. Williams, A. Kennedy, E. Waters, A.M. Pesenacker, B. Soskic, C. Hinze, T.Z. Hou, B. Rowshanravan, D. Janman, L.S.K. Walker, D.M. Sansom, CD86 is a selective CD28 ligand supporting FoxP3+ regulatory T cell homeostasis in the presence of high levels of CTLA-4, Front. Immunol. 11 (2020) 600000, https://doi.org/10.3389/fimmu.2020.600000.
[2] P.A. Roche, K. Furuta, The ins and outs of MHC class II-mediated antigen processing and presentation, Nat. Rev. Immunol. 15 (2015) 203–216, https://doi.org/10.1038/nri3818.
[3] R.V. Luckheeram, R. Zhou, A.D. Verma, B. Xia, CD4^{+} T cells: differentiation and functions, Clin. Dev. Immunol. 2012 (2012) 1–12, https://doi.org/10.1155/2012/925135.
[4] J. Zhu, W.E. Paul, CD4 T cells: fates, functions, and faults, Blood 112 (2008) 1557–1569, https://doi.org/10.1182/blood-2008-05-078154.
[5] J.S. Cho, E.M. Pietras, N.C. Garcia, R.I. Ramos, D.M. Farzam, H.R. Monroe, J. E. Magorien, A. Blauvelt, J.K. Kolls, A.L. Cheung, G. Cheng, R.L. Modlin, L. S. Miller, IL-17 is essential for host defense against cutaneous Staphylococcus aureus infection in mice, J. Clin. Investig. 120 (2010) 1762–1773, https://doi.org/10.1172/JCI40891.

[6] S. Rutz, W. Ouyang, Regulation of Interleukin-10 expression, in: X. Ma (Ed.), Regul. Cytokine Gene Expr. Immun. Dis., Springer, Netherlands, Dordrecht, 2016, pp. 89–116, https://doi.org/10.1007/978-94-024-0921-5_5.
[7] J.M. Rojas, M. Avia, V. Martín, N. Sevilla, IL-10: a multifunctional cytokine in viral infections, J. Immunol. Res. 2017 (2017) 6104054, https://doi.org/10.1155/2017/6104054.
[8] T. Inamoto, K. Furuta, C. Han, M. Uneme, T. Kano, K. Ishikawa, C. Kaito, Short-chain fatty acids stimulate dendrite elongation in dendritic cells by inhibiting histone deacetylase, FEBS J. 290 (2023) 5794–5810, https://doi.org/10.1111/febs.16945.
[9] R. Rohatgi, H.H. Ho, M.W. Kirschner, Mechanism of N-Wasp activation by Cdc42 and phosphatidylinositol 4,5-Bisphosphate, J. Cell Biol. 150 (2000) 1299–1310, https://doi.org/10.1083/jcb.150.6.1299.
[10] L. Ma, R. Rohatgi, M.W. Kirschner, The Arp2/3 complex mediates actin polymerization induced by the small GTP-binding protein Cdc42, Proc. Natl. Acad. Sci. 95 (1998) 15362–15367, https://doi.org/10.1073/pnas.95.26.15362.
[11] F. Korobova, T. Svitkina, Arp2/3 complex is important for filopodia formation, growth cone motility, and neuritogenesis in neuronal cells, Mol. Biol. Cell 19 (2008) 1561–1574, https://doi.org/10.1091/mbc.e07-09-0964.
[12] L. Liu, L. Zhang, S. Zhao, X.-Y. Zhao, P.-X. Min, Y.-D. Ma, Y.-Y. Wang, Y. Chen, S.-J. Tang, Y.-J. Zhang, J. Du, L. Gu, Non-canonical notch signaling regulates actin remodeling in cell migration by activating PI3K/AKT/Cdc42 pathway, Front. Pharmacol. 10 (2019) 370, https://doi.org/10.3389/fphar.2019.00370.
[13] Y. Qian, L. Corum, Q. Meng, J. Blenis, J.Z. Zheng, X. Shi, D.C. Flynn, B.-H. Jiang, PI3K induced actin filament remodeling through akt and p70S6K1: implication of essential role in cell migration, Am. J. Physiol.-Cell Physiol. 286 (2004) C153–C163, https://doi.org/10.1152/ajpcell.00142.2003.
[14] M.J. Gasson, Plasmid complements of Streptococcus lactis NCDO 712 and other lactic streptococci after protoplast-induced curing, J. Bacteriol. 154 (1983) 1–9, https://doi.org/10.1128/jb.154.1.1-9.1983.
[15] E.S. Duthie, L.L. Lorenz, Staphylococcal coagulase; mode of action and antigenicity, J. Gen. Microbiol. 6 (1952) 95–107, https://doi.org/10.1099/00221287-6-1-2-95.
[16] T. Ueda, C. Kaito, Y. Omae, K. Sekimizu, Sugar-responsive gene expression and the agr system are required for colony spreading in Staphylococcus aureus, Microb. Pathog. 51 (2011) 178–185, https://doi.org/10.1016/j.micpath.2011.04.003.
[17] C. Kaito, Y. Saito, G. Nagano, M. Ikuo, Y. Omae, Y. Hanada, X. Han, K. Kuwahara-Arai, T. Hishinuma, T. Baba, T. Ito, K. Hiramatsu, K. Sekimizu, Transcription and translation products of the cytolysin gene psm-mec on the Mobile genetic element SCCmec regulate Staphylococcus aureus virulence, PLoS Pathog. 7 (2011) e1001267, https://doi.org/10.1371/journal.ppat.1001267.
[18] Y. Katoh, S. Michisaka, S. Nozaki, T. Funabashi, T. Hirano, R. Takei, K. Nakayama, Practical method for targeted disruption of cilia-related genes by using CRISPR/Cas9-mediated, homology-independent knock-in system, Mol. Biol. Cell 28 (2017) 898–906, https://doi.org/10.1091/mbc.E17-01-0051.
[19] K. Furuta, K. Miyazato, K. Kobata, K. Ishikawa, C. Kaito, 1,2-naphthoquinone enhances IFN-γ-induced MHC-I expression in dendritic cells, thereby inducing CD8 T cell activation, Biochem. Biophys. Res. Commun. 779 (2025) 152453, https://doi.org/10.1016/j.bbrc.2025.152453.
[20] K. Furuta, H. Onishi, Y. Ikada, K. Masaki, S. Tanaka, C. Kaito, ATP and its metabolite adenosine cooperatively upregulate the antigen-presenting molecules on dendritic cells leading to IFN-γ production by T cells, J. Biol. Chem. 299 (2023) 104587, https://doi.org/10.1016/j.jbc.2023.104587.
[21] M.A. Armant, M.J. Fenton, Toll-like receptors: a family of pattern-recognition receptors in mammals, Genome Biol. 3 (2002), https://doi.org/10.1186/gb-2002-3-8-reviews3011 reviews3011.1-reviews311.6.
[22] R. Schwandner, R. Dziarski, H. Wesche, M. Rothe, C.J. Kirschning, Peptidoglycan- and lipoteichoic acid-induced cell activation is mediated by toll-like receptor 2, J. Biol. Chem. 274 (1999) 17406–17409, https://doi.org/10.1074/jbc.274.25.17406.
[23] A. Mansouri, I. Akthar, A. Miyamoto, TLR2 and TLR4 bridge physiological and pathological inflammation in the reproductive system, Commun. Biol. 8 (2025) 1008, https://doi.org/10.1038/s42003-025-08424-x.
[24] Y. Chen, Z. Huang, X. Chen, H. Ye, Activation of the toll-like receptor 2 signaling pathway inhibits the proliferation of HCC cells in vitro, Oncol. Rep. 42 (2019) 2267–2278, https://doi.org/10.3892/or.2019.7340.
[25] K.J. Brandt, C. Fickentscher, E.K.O. Kruithof, P. de Moerloose, TLR2 ligands induce NF-κB activation from endosomal compartments of human monocytes, PLoS One 8 (2013) e80743, https://doi.org/10.1371/journal.pone.0080743.
[26] C.A. Leifer, A.E. Medvedev, Molecular mechanisms of regulation of toll-like receptor signaling, J. Leukoc. Biol. 100 (2016) 927–941, https://doi.org/10.1189/jlb.2MR0316-117RR.
[27] J.L. D'Agostino, B.L. Goode, Dissection of Arp2/3 complex actin nucleation mechanism and distinct roles for its nucleation-promoting factors in Saccharomyces cerevisiae, Genetics 171 (2005) 35–47, https://doi.org/10.1534/genetics.105.040634.
[28] R. Rohatgi, L. Ma, H. Miki, M. Lopez, T. Kirchhausen, T. Takenawa, M. W. Kirschner, The interaction between N-WASP and the Arp2/3 complex links Cdc42-dependent signals to actin assembly, Cell 97 (1999) 221–231, https://doi.org/10.1016/s0092-8674(00)80732-1.
[29] S. Zheng, F. Qin, J. Yin, D. Li, Y. Huang, L. Hu, L. He, C. Lv, X. Li, S. Li, W. Hu, Role and mechanism of actin-related protein 2/3 complex signaling in cancer invasion and metastasis: a review, Medicine (Baltim.) 102 (2023) e33158, https://doi.org/10.1097/MD.0000000000033158.
[30] T. Yoshimura, Y. Kawano, N. Arimura, S. Kawabata, A. Kikuchi, K. Kaibuchi, GSK-3beta regulates phosphorylation of CRMP-2 and neuronal polarity, Cell 120 (2005) 137–149, https://doi.org/10.1016/j.cell.2004.11.012.
[31] Y.T. Kim, E.-M. Hur, W.D. Snider, F.-Q. Zhou, Role of GSK3 signaling in neuronal morphogenesis, Front. Mol. Neurosci. 4 (2011) 48, https://doi.org/10.3389/fnmol.2011.00048.
[32] A. Atrih, G. Bacher, G. Allmaier, M.P. Williamson, S.J. Foster, Analysis of peptidoglycan structure from vegetative cells of Bacillus subtilis 168 and role of PBP 5 in peptidoglycan maturation, J. Bacteriol. 181 (1999) 3956–3966, https://doi.org/10.1128/JB.181.13.3956-3966.1999.
[33] M.-P. Chapot-Chartier, S. Kulakauskas, Cell wall structure and function in lactic acid bacteria, Microb. Cell Fact. 13 (Suppl 1) (2014) S9, https://doi.org/10.1186/1475-2859-13-S1-S9.
[34] S. Sharif, M. Singh, S.J. Kim, J. Schaefer, Staphylococcus aureus peptidoglycan tertiary structure from carbon-13 spin diffusion, J. Am. Chem. Soc. 131 (2009) 7023–7030, https://doi.org/10.1021/ja808971c.
[35] E.J. Hayhurst, L. Kailas, J.K. Hobbs, S.J. Foster, Cell wall peptidoglycan architecture in Bacillus subtilis, Proc. Natl. Acad. Sci. U. S. A 105 (2008) 14603–14608, https://doi.org/10.1073/pnas.0804138105.
[36] F. Sallusto, M. Cella, C. Danieli, A. Lanzavecchia, Dendritic cells use macropinocytosis and the mannose receptor to concentrate macromolecules in the major histocompatibility complex class II compartment: downregulation by cytokines and bacterial products, J. Exp. Med. 182 (1995) 389–400, https://doi.org/10.1084/jem.182.2.389.
[37] Z. Liu, P.A. Roche, Macropinocytosis in phagocytes: regulation of MHC class-II-restricted antigen presentation in dendritic cells, Front. Physiol. 6 (2015) 1, https://doi.org/10.3389/fphys.2015.00001.
[38] S.E. Doyle, R.M. O'Connell, G.A. Miranda, S.A. Vaidya, E.K. Chow, P.T. Liu, S. Suzuki, N. Suzuki, R.L. Modlin, W.-C. Yeh, T.F. Lane, G. Cheng, Toll-like receptors induce a phagocytic gene program through p38, J. Exp. Med. 199 (2004) 81–90, https://doi.org/10.1084/jem.20031237.
[39] M.A. West, R.P.A. Wallin, S.P. Matthews, H.G. Svensson, R. Zaru, H.-G. Ljunggren, A.R. Prescott, C. Watts, Enhanced dendritic cell antigen capture via toll-like receptor-induced actin remodeling, Science 305 (2004) 1153–1157, https://doi.org/10.1126/science.1099153.
[40] C.D. Platt, J.K. Ma, C. Chalouni, M. Ebersold, H. Bou-Reslan, R.A.D. Carano, I. Mellman, L. Delamarre, Mature dendritic cells use endocytic receptors to capture and present antigens, Proc. Natl. Acad. Sci. U. S. A 107 (2010) 4287–4292, https://doi.org/10.1073/pnas.0910609107.
[41] D.M. Elizondo, T.E. Andargie, N.L. Haddock, T.A. Boddie, M.W. Lipscomb, Drebrin 1 in dendritic cells regulates phagocytosis and cell surface receptor expression through recycling for efficient antigen presentation, Immunology 156 (2019) 136–146, https://doi.org/10.1111/imm.13010.
[42] N. Morita, E. Umemoto, S. Fujita, A. Hayashi, J. Kikuta, I. Kimura, T. Haneda, T. Imai, A. Inoue, H. Mimuro, Y. Maeda, H. Kayama, R. Okumura, J. Aoki, N. Okada, T. Kida, M. Ishii, R. Nabeshima, K. Takeda, GPR31-dependent dendrite protrusion of intestinal CX3CR1+ cells by bacterial metabolites, Nature 566 (2019) 110–114, https://doi.org/10.1038/s41586-019-0884-1.
[43] J. Farache, I. Koren, I. Milo, I. Gurevich, K.-W. Kim, E. Zigmond, G.C. Furtado, S. A. Lira, G. Shakhar, Luminal bacteria recruit CD103+ dendritic cells into the intestinal epithelium to sample bacterial antigens for presentation, Immunity 38 (2013) 581–595, https://doi.org/10.1016/j.immuni.2013.01.009.
[44] J.H. Cummings, E.W. Pomare, W.J. Branch, C.P. Naylor, G.T. Macfarlane, Short chain fatty acids in human large intestine, portal, hepatic and venous blood, Gut 28 (1987) 1221–1227, https://doi.org/10.1136/gut.28.10.1221.
[45] R.J. Murray, Recognition and management of Staphylococcus aureus toxin-mediated disease, Intern. Med. J. 35 (Suppl 2) (2005) S106–S119, https://doi.org/10.1111/j.1444-0903.2005.00984.x.
[46] J.C. McNeil, Staphylococcus aureus - antimicrobial resistance and the immunocompromised child, Infect. Drug Resist. 7 (2014) 117–127, https://doi.org/10.2147/IDR.S39639.
[47] J.M. Kwiecinski, A.R. Horswill, Staphylococcus aureus bloodstream infections: pathogenesis and regulatory mechanisms, Curr. Opin. Microbiol. 53 (2020) 51–60, https://doi.org/10.1016/j.mib.2020.02.005.
[48] M.J. McGeachy, D.J. Cua, S.L. Gaffen, The IL-17 family of cytokines in health and disease, Immunity 50 (2019) 892–906, https://doi.org/10.1016/j.immuni.2019.03.021.
[49] A. Chaudhry, R.M. Samstein, P. Treuting, Y. Liang, M.C. Pils, J.-M. Heinrich, R. S. Jack, F.T. Wunderlich, J.C. Brüning, W. Müller, A.Y. Rudensky, Interleukin-10 signaling in regulatory T cells is required for suppression of Th17 cell-mediated inflammation, Immunity 34 (2011) 566–578, https://doi.org/10.1016/j.immuni.2011.03.018.